Journal of Alloys and Compounds 839 (2020) 155085

Contents lists available at ScienceDirect

Journal of Alloys and Compounds

journal homepage: http://www.elsevier.com/locate/jalcom

Anisotropy of piezocaloric effect at ferroelectric phase transitions in ammonium hydrogen sulphate

Ekaterina A. Mikhaleva [a], Mikhail V. Gorev [a, b], Maxim S. Molokeev [a, b, c], Andrey V. Kartashev [a, d], Igor N. Flerov [a, b, *]

[a] Kirensky Institute of Physics, Federal Research Center KSC SB RAS, 660036, Krasnoyarsk, Russia
[b] Institute of Engineering Physics and Radioelectronics, Siberian Federal University, 660074, Krasnoyarsk, Russia
[c] Department of Physics, Far Eastern State Transport University, 680021, Khabarovsk, Russia
[d] Astafijev Krasnoyarsk State Pedagogical University, 660049, Krasnoyarsk, Russia

ARTICLE INFO

Article history:
Received 8 July 2019
Received in revised form
26 February 2020
Accepted 6 April 2020
Available online 8 May 2020

Keywords:
Piezocaloric effect
Phase transition
Ferroelectrics
Thermal expansion
High-pressure
Entropy

ABSTRACT

The role of anisotropy of the thermal expansion in formation of piezocaloric effect (PCE) near ferroelectric phase transitions in NH_4HSO_4 was studied. Strong difference in linear baric coefficients and as a result in intensive and extensive PCE associated with the different crystallographic axes was found. PCE giving the main contribution to the barocaloric effect were determined at both phase transitions. Rather strong effect of the lattice dilatation on the tuning of PCE was observed. Comparative analysis of PCE at the phase transitions in different materials showed that NH_4HSO_4 can be considered as a promising solid-state refrigerant. A hypothetical cooling cycle based on alternate using uniaxial pressure along two axes was considered.

1. Introduction

Solids exhibiting high caloric effects (CE) attract a great attention of both researches and engineers due a possibility to use them as effective solid-state refrigerants at designing alternative cooling cycles [1–5]. Different CE exist according to their physical nature: magnetocaloric (MCE), electrocaloric (ECE), barocaloric (BCE), piezo-(or elasto-)caloric PCE(ElCE), flexocaloric (FCE). All these effects are associated with a reversible change in the adiabatic temperature (ΔT_{AD}) or isothermal entropy (ΔS_{CE}) of the material when the corresponding external field is applied or removed.

Studies of caloric materials are mainly carried out in two directions. The former is related to the search for solids competitive in caloric efficiency relative to gas coolants used in traditional large-scale gas-compressor refrigerators. In such a case, materials with significant intensive, ΔT_{AD}, and extensive, ΔS_{CE}, MCE and BCE look like the most promising [2,6,7].

The main objective of the latter direction is to create solid refrigerants that can be used in miniature refrigerators, essential for modern micro- and nanoelectronic devices with large heat emission [8]. Obviously, for this purpose, the most suitable are single crystal or ceramic dielectric materials that do not require bulky external devices for the implementation of individual or pairing CE: ECE, PCE (ElCE), FCE. The disadvantages of ECE and FCE are associated, first, with the irreversible process of Joule heat generation in a ferroelectric when high electric field is applied and, second, with a significant nonlinear deformation of the caloric element which is not very convenient, for example, when designing combined working elements of the microcircuit–refrigerator.

PCE can be considered as a special case of the bulk BCE, coupled with hydrostatic pressure, and is realized under the influence of uniaxial mechanical stress σ:

* Corresponding author. Kirensky Institute of Physics, Federal Research Center KSC SB RAS, 660036, Krasnoyarsk, Russia.
E-mail addresses: katerina@iph.krasn.ru (E.A. Mikhaleva), gorev@iph.krasn.ru (M.V. Gorev), msmolokeev@mail.ru (M.S. Molokeev), akartashev@yandex.ru (A.V. Kartashev), flerov@iph.krasn.ru (I.N. Flerov).

https://doi.org/10.1016/j.jallcom.2020.155085
0925-8388/

$$\Delta S_{PCE} = -\int V_m(T,\sigma)\alpha(T,\sigma)d\sigma;\ \ \Delta T_{AD}^{PCE} = -\frac{T}{C_p}\Delta S_{PCE}, \quad (1)$$

where V_m is the molar volume and $\alpha = l^{-1}(\partial l/\partial T)_\sigma$ is a linear thermal expansion coefficient.

For the first time experimental studies of PCE were carried out by Joule in the 19th century [9]. He performed the measurements at room temperature and found that the response of the temperature of the samples under stress depends on the type of material (wood, metals. etc.) as well as the magnitude of the tensile/compressive load and is rather small, mainly due to the small values of the coefficient α of the materials studied.

It is known, however, that thermal expansion can significantly increase in the region of phase transition of various physical origin. The reason is that linear/volume strain either is itself an order parameter (ferroelastic and martensitic transformations) or is strongly related to the principal order parameter of a different nature (magnetization, polarization). In both cases, a pronounced anomalous behavior of the coefficient α is observed in the vicinity of the transition point.

In recent years, much attention has been paid to the study of PCE in shape memory alloys undergoing the martensitic transformations accompanied by large entropy change [10–13]. Rather low tensile and compressive stresses created in the samples in the form of wire or ribbon led to significant values of ΔT_{AD} and ΔS_{CE} in some materials [14,15].

However, in the case of alloys, PCE was measured only in one direction. On the other hand, as can be seen from Eq. (1), it is obvious that in anisotropic materials, the magnitude and sign of PCE can be different in accordance with the difference in the α coefficients along different directions. Recently, we have proved this assumption studying PCE near ferroelastic phase transitions in some orthorhombic single crystals [16,17]. It was found that anisotropy of the crystal lattice allows one to realize conventional ($\Delta T_{AD} > 0, \Delta S_{CE} < 0$) and inverse ($\Delta T_{AD} < 0, \Delta S_{CE} > 0$) PCE in the same sample using uniaxial stresses applying along different crystallographic axes. We have also demonstrated that in some case the values of the uniaxial CE can be comparable with BCE or even exceed it.

PCE in some ferroelectrics (ceramics, films and single crystals) was studied experimentally and in the scope of some theoretical approaches only to a small extent [18–21]. Moreover, in these materials the effect was also considered only for one direction in the sample and never the attention was paid to the anisotropy of PCE.

Analysis performed recently by U.S. Department of Energy showed that studies of thermoelastic effects (PCE and BCE) in solids are the most promising in terms of the development of alternative cooling technologies [22].

In the present paper, we analyzed the effect of anisotropy of thermal expansion on the intensive and extensive piezocaloric efficiency of ferroelectric NH_4HSO_4 using method developed by us earlier [16,17]. Ammonium hydrogen sulphate was chosen as very convenient model object due to its peculiar and interesting properties. Firstly, it undergoes the succession of two phase transitions $P2_1/c$ (T_1=271 K)↔ Pc (T_2=159 K)↔ $P1$, of the second and first order, respectively [23]. Secondly, these transformations also differ greatly from each other by entropy (ΔS_1=1.2 J/mol·K, ΔS_2 = 6.7 J/mol·K) and sensitivity to hydrostatic pressure (dT_1/dp=+90± 15 K/GPa and dT_2/dp = -123±15 K/GPa). Thirdly, strong effect of the hydrostatic pressure on the entropy jump associated with the first order phase transition at T_2 was observed but information on the temperature hysteresis was absent. Fourthly, far from the phase transition points, NH_4HSO_4 is characterized by rather large coefficient of the volume thermal expansion of the crystal lattice, β_{LAT}=(1.5–2.0)·10^{-4} K^{-1}. In accordance with [24], this can significantly effects on BCE. However, the question of the influence of thermal expansion of the crystal lattice on PCE in ferroelectrics remained open.

Taking in mind the points above, we performed detailed experimental study of linear thermal expansion near both phase transition in NH_4HSO_4 as well as hysteretic phenomena around T_2.

2. Experimental

Rather large single crystals of NH_4HSO_4 were grown by slow evaporation at 45 from aqueous solution containing equimolar quantities of $(NH_4)_2SO_4$ and H_2SO_4.

XRD examination of the quality of the sample at room temperature was performed with a Bruker D8 ADVANCE powder diffractometer (Cu-Kα radiation), TTK 450 Anton Paar heat attachment and linear VANTEC detector. It revealed, firstly, a monoclinic symmetry (sp. gr. $P2_1/c$, Z = 8), consistent with suggested in Refs. [23,25,26] and, secondly, the absence of any additional phases. Fig. 1 shows the results of Rietveld refinement (R_{wp}=6.04, R_p = 4.23, χ^2 = 2.06).

A good agreement was found between the unit cell parameters in the sample under study (a = 14.3954 (7)Å, b = 4.5938 (2)Å, c = 14.8343 (8)Å, β = 120.883 (2) grad) and those determined earlier in Ref. [25,26].

Further experimental procedure was organized taking in mind the peculiarities of the phase transitions in NH_4HSO_4, Due to a large volume change in the region of the first order phase transition $Pc \leftrightarrow P1$, detected when measuring on quasi-ceramic samples prepared using the solution and melt technology [23], we assumed that single-crystal samples may crack during experiments with heat treatments around T_2.

Therefore, experimental studies were carried out in several stages. At the first stage, the behavior of linear thermal expansion was studied on single-crystal specimen in the range from 175 K to 320 K including the vicinity of the second order phase transition $P2_1/c \leftrightarrow Pc$. The NH_4HSO_4 sample was cut in the form of rectangular prism with the dimensions of 7.4 × 8.6 × 5.9 mm^3 along crystallographic axes a, b, c for the pseudo-orthorhombic cell. Measurements were performed in a vacuum atmosphere (~10^{-2} mm Hg)

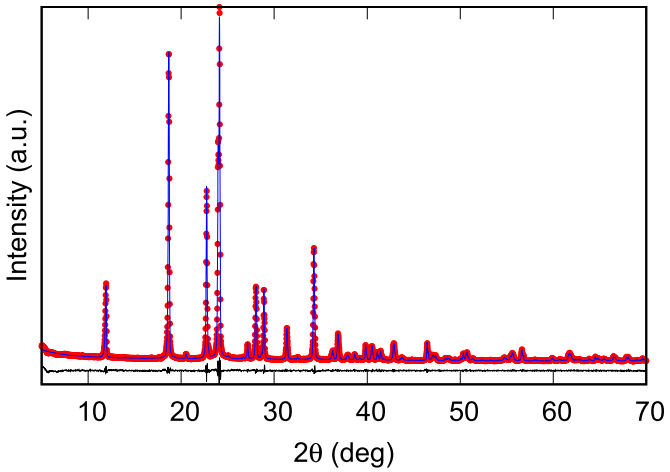

Fig. 1. Rietveld analysis patterns for X-ray powder diffraction of NH_4HSO_4 at room temperature. Red dots are experimental data. The blue solid line corresponds to the calculated intensities. The black line below the profiles stand for the difference between the observed and calculated intensities. (For interpretation of the references to colour in this figure legend, the reader is referred to the Web version of this article.)

using a quartz optic-mechanical dilatometer with a sensitivity of 1.2×10^{-6} cm. Temperature step of discrete heating was ≤0.5 K and ≥2 K near and far from T_1, respectively.

At the second stage, the same sample was examined using an a homemade adiabatic calorimeter [27] in continuous cooling/heating mode through the phase transition $Pc \leftrightarrow P1$ at a very low temperature variation rate of about $dT/dt = \pm 10^{-3}$ K/min. It was found that, indeed, single-crystal sample was cracked after cooling/heating through the phase transition $Pc \leftrightarrow P1$. Thus, we were unable to measure the linear expansion of the NH_4HSO_4 single-crystal around T_2 using a quartz dilatometer.

Therefore, at the next stage, X-ray studies were performed on a powder sample to get information on the temperature behavior of the unit cell parameters. Measurements were carried out in the temperature range from 155 K to 180 K with the step of about 1 K.

3. Results and discussion

First of all it is worth to discuss the hysteretic phenomena observed in calorimetric experiments near T_2. The hysteresis of the phase transition temperature was found of about $\delta T_2 = 2.5$ K. The entropy jump δS_2 decreases with pressure increase and is equal to zero at rather low pressure of the tricritical point $p_{tcp} \approx 0.18 \pm 0.02$ GPa [23]. The rapid approach of the phase transition under pressure to the tricritical point accompanied by $\delta T_2 \rightarrow 0$ is an important property of NH_4HSO_4 and can be considered as very useful for the implementation of a reliable and stable BCE and PCE [3].

The temperature dependencies of the linear thermal expansion coefficients, α_i, in the vicinity T_1 and unit cell parameters, a_i, around T_2 are shown in Fig. 2 (a) and (b). X-ray data are also presented for the pseudo-orthorhombic cell. It can be seen that far from the phase transition points, NH_4HSO_4 is characterized by a positive thermal dilatation in all crystallographic directions. The values of α_i evaluated at 180 K from dependencies of $a_i(T)$ ($\alpha_a = +(7.5 \pm 0.8) \cdot 10^{-5}$ K^{-1}; $\alpha_b = +(3.5 \pm 0.5) \cdot 10^{-5}$ K^{-1}; $\alpha_c = +(6.4 \pm 0.7) \cdot 10^{-5}$ K^{-1}) agree well with coefficients determined in dilatometric experiments (Fig. 2(a)).

A highly anisotropic anomalous behavior of thermal expansion was found at both T_1 and T_2. The jumps at the phase transition points of the linear expansion coefficients, $\delta\alpha_i = \alpha_i - \alpha_i^{LAT}$ (α_i^{LAT} is a lattice contribution), and linear strains, $\delta(\Delta a_i/a_i) = (\Delta a_i/a_i)_{T>T2} - (\Delta a_i/a_i)_{T<T2}$, are presented in Table 1.

Different signs of $\delta\alpha_i$ and $\delta(\Delta a_i/a_i)$ values associated with different axes indicate that in accordance with Eq. 1, PCE can be realized as conventional or inverse. Summation of the jumps of the unit cell parameters, $\sum \delta(\Delta a_i/a_i) = \delta(\Delta V/V)$, and linear expansion coefficients, $\sum \delta\alpha_i = \delta\beta$, show that jumps in volume strain and coefficient β, at T_2 and T_1, respectively, have different signs and this determines the difference of signs of baric coefficients for the phase transitions in ammonium hydrogen sulphate (dT_2/dp=-123 K/GPa; $dT_1/dp = 90$ K/GPa) [23].

Table 1
Some parameters of the thermal expansion at the phase transition points T_1 and T_2 in NH_4HSO_4. $\delta\alpha_i$ and $\delta\beta$ – jumps of the linear and volume expansion coefficients. $\delta a_i/a_i$ and $\delta V/V$ – jumps of parameters and volume of the unit cell. $dT/d\sigma_i$ and (dT/dp) – shift of the phase transition temperatures under uniaxial and hydrostatic pressure.

	$P2_1/c \leftrightarrow Pc$	$Pc \leftrightarrow P1$	Ref.
$\delta\alpha_a \cdot 10^6$,K^{-1}	+(25.5±1.0)		
$\delta\alpha_b \cdot 10^6$,K^{-1}	+(64.5±3.0)		
$\delta\alpha_c \cdot 10^6$,K^{-1}	-(8.0±0.5)		
$\delta\beta \cdot 10^6$,K^{-1}	+(82.0±4.5)		
$\delta a/a$, %		+(0.69±0.03)	
$\delta b/b$, %		-(0.52±0.02)	
$\delta c/c$, %		-(1.27±0.06)	
$\delta V/V$, %		-(1.10±0.11)	
$dT_1/d\sigma_a$, K·GPa^{-1}	+(33±5)		
$dT_1/d\sigma_b$, K·GPa^{-1}	+(79±10)		
$dT_1/d\sigma_c$, K·GPa^{-1}	-(10±3)		
$(dT_1/dp)_{calc}$, K·GPa^{-1}	+(10,2±18)		
$(dT_1/dp)_{exp}$, K·GPa^{-1}	+(90±15)		[23]
$dT_2/d\sigma_a$, K·GPa^{-1}		+(45 ± 4)	
$dT_2/d\sigma_b$, K·GPa^{-1}		-(50±5)	
$dT_2/d\sigma_c$, K·GPa^{-1}		-(122±7)	
$(dT_2/dp)_{calc}$, K·GPa^{-1}		-(12,7±16)	
$(dT_2/dp)_{exp}$, K·GPa^{-1}		-(12,3±15)	[23]

Sensitivity of the phase transition temperatures in NH_4HSO_4 to uniaxial stress, $dT_1/d\sigma_i$ and $dT_2/d\sigma_i$, was determined in the scope of the Ehrenfest, $dT_1/d\sigma_i = T \cdot \delta\alpha_i/\delta C_p$, and Clapeiron–Clausius, $dT_2/d\sigma_i = \delta(\Delta a_i/a_i)/\delta S$, relations using data on the jumps in entropy δS, heat capacity δC_p [23], linear strain $\delta(\Delta a_i/a_i)$ and coefficient of the linear thermals expansion $\delta(\Delta\alpha_i)$. The results of calculations are presented in (Table 1). It is evident that in accordance with the strong anisotropy of the thermal dilatation there is a large difference in the values and signs of the coefficients $dT/d\sigma_i$. Table 1 also demonstrates that the largest values of $dT/d\sigma_i$ at T_1 and T_2 are, firstly, related to different crystallographic axes, and secondly, they are the largest contributors to the dT_1/dp and dT_2/dp values. The reliability of the data obtained is confirmed by a good agreement of the calculated, $(dT/dp)_{calc}$ and experimentally determined $(dT/dp)_{exp}$ baric coefficients (Table 1).

In order to determine the intensive and extensive PCE in NH_4HSO_4, we used previously obtained results of the separation of

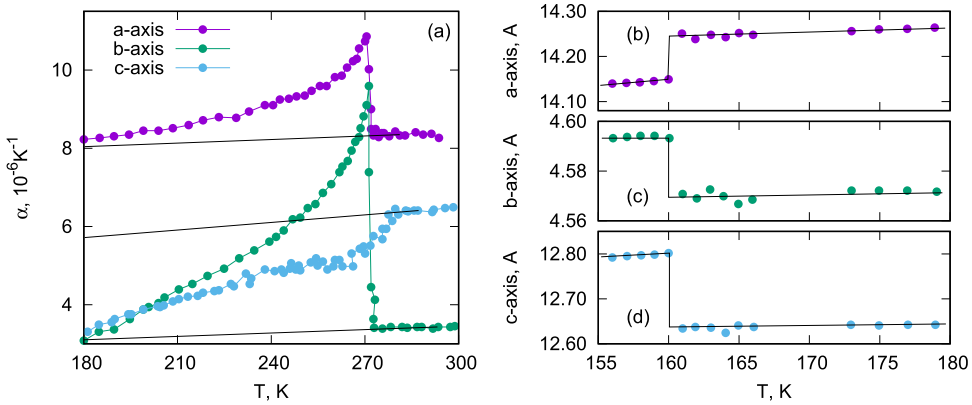

Fig. 2. Temperature dependencies of (a) thermal expansion coefficients α_i near T_1 and (b,c,d) cell parameters a, b and c for the pseudo-orthorhombic cell near T_2 in NH_4HSO_4.

the anomalous, $\Delta S_1(T)$ and $\Delta S_2(T)$, and lattice, S_{LAT}, entropies at $p = 0$ [23]. It was mentioned above that at $p \approx 0.2$ GPa the phase transition at T_2 exhibits a tricritical behavior with $\delta S_2 = 0$. Both structural units SO_4^{2-} and NH_4^+ were defined as disordered and totally ordered in the initial $P2_1/c$, and final, $P1$, phases, respectively [26]. Since we did not find any triple points in the $T-p$ phase diagram, the symmetries of all phases in NH_4HSO_4 are preserved under pressure. Due to the relationship between symmetry and the degree of disordering, the latter is also retained and, as a result, the entropies ΔS_1 and ΔS_2 remain unchanged, at least under the pressure used in the present studies.

The total entropy as a function of temperature, $S(T)$, at different $\sigma_i > 0$ was determined by summation of S_{LAT} and anomalous contributions $\Delta S_1(T)$ as well as $\Delta S_2(T)$ at $\sigma_i = 0$ shifted along the temperature scale according to the values of $dT_1/\,d\sigma_i$ and $dT_2/\,d\sigma_i$.

$$S(T,\sigma_i) = S_{LAT}(T) + \Delta S_1(T + (dT_1/\,d\sigma_i)\sigma_i) + \Delta S_2(T + (dT_2/\,d\sigma_i)\sigma_i) \quad (2)$$

It should be noted that this procedure was carried out at two different conditions: first, without taking into account, and second, taking into account the thermal expansion of the crystal lattice. In the latter case, the lattice entropy change under pressure was determined using Maxwell relation $(\partial S_{LAT}/\partial\sigma_i)_T = (\partial(\Delta a_i/a_i)/\partial T)_{\sigma_i}$.

$$\Delta S_{LAT}^{PCE}(T,\sigma_i) = -V_m \int \left(\frac{\partial(\Delta a_i/a_i)}{\partial T}\right)_{\sigma_i} d\sigma_i \approx -V_m \cdot \alpha_{LAT}(T) \cdot \Delta\sigma_i. \quad (3)$$

The results of both procedures are shown in Fig. 3 for two external mechanical stresses, 0.05 and 0.1 GPa.

When lattice expansion was not taken into account, the extensive PCE under stress along different axes was determined as a difference $\Delta S_{PCE}(T,\sigma_i) = S(T,\sigma_i) - S(T,\sigma_i = 0)$ at constant temperature. The temperature dependencies of the intensive PCE were revealed analyzing plots of $S(T,\sigma_i) = S_{LAT}(T,\sigma_i = 0) + \Delta S(T,\sigma_i)$ at constant entropy $S(T,\sigma_i) = S(T + \Delta T_{AD},\sigma_i = 0)$. Fig. 4(a)-(d), 5(a)-(d) and 6(a)-(d) show the behavior of PCE associated with the main crystallographic axes in the region of both phase transitions. In accordance with the sign of $dT_1/d\sigma_i$ and $dT_2/d\sigma_i$ (Table 1), PCE can be conventional and inverse.

In the case of the phase transition at T_1, the maximum possible value of the extensive PCE equal to the entropy of the phase transition $\Delta S_1 = 1.2$ J/mol K has not been achieved even at $\sigma_i = 0.4$ GPa. Due to the most pronounced sensitivity of T_1 to σ_b (Table 1), NH_4HSO_4 shows at all pressures the largest values of PCE under stress along the b axis.

The values of the extensive PCE around T_2 for all axes are rather close to the maximum value $(\Delta S_{PCE})_{max} = \Delta S_2 = 6.7$ J/mol·K and can be realized at almost identical very low uniaxial pressures < 0.05 GPa. However, to achieve the maximum magnitude of the intensive PCE, $(\Delta T_{AD}^{\sigma_i})_{max} \approx 10$ K, significantly greater mechanical stresses are needed: $\sigma_a \approx \sigma_b \approx 0.3$ GPa, $\sigma_c \approx 0.1$ GPa, The slower saturation of ΔT_{AD} under pressure is due to its strong dependence on two circumstances: first, on the derivative dS_{LAT}/dT and, second, on the baric coefficient $dT/d\sigma$.

Let us consider now the contribution of the lattice dilatation to the piezocaloric efficiency of NH_4HSO_4. Due to the positive sign of $(\alpha_i)_{LAT}$ along all axes, PCE_{LAT} is always conventional. Fig. 3 (c), (d) show that the greatest decrease in $S(T,\sigma_a)$ is associated with the largest magnitude of $(\alpha_a)_{LAT}$. At $p = 0.1$ GPa, the decrease in $S(T,\sigma_i)$ is about 0.5% and 1% near T_1 and T_2, respectively, and increases with pressure increase. As a result, extensive and intensive PCE undergo significant changes during both phase transitions.

At the transformation $P2_1/c \leftrightarrow Pc$, strong increase in both PCE was observed: at $\sigma = 0.4$ GPa, along all axes. The value ΔS_{PCE} exceeds the entropy of the phase transition more than twice and ΔT_{AD} also becomes very large (>5 K with σ_a). One can also see that taking into account the lattice dilatation is accompanied by a change in PCE along the c axis from the inverse to the conventional (Fig. 6 (e), (f)).

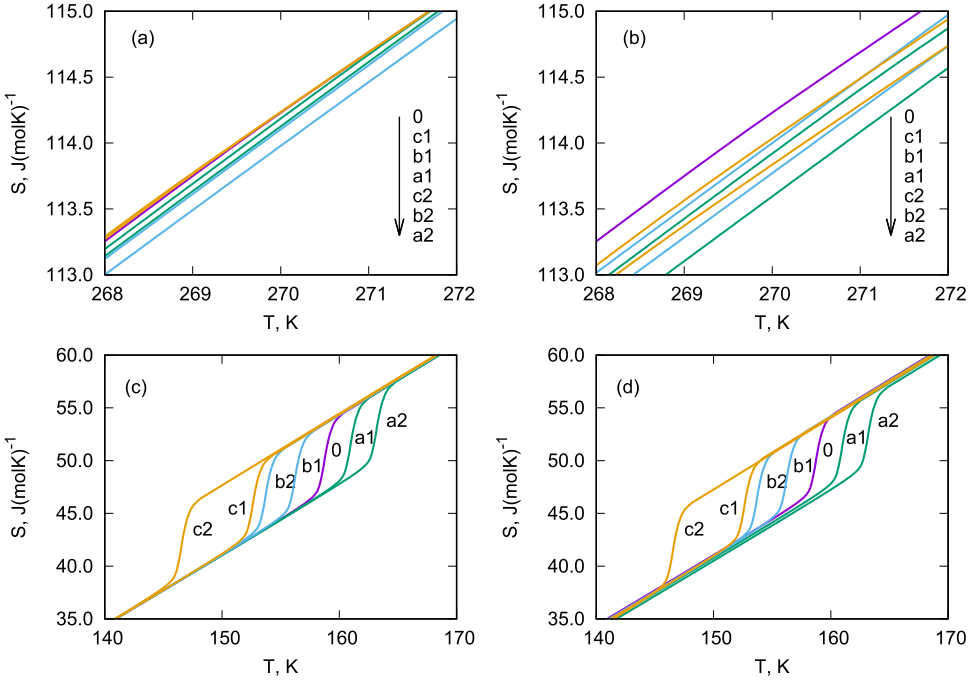

Fig. 3. Temperature dependencies of total entropy of NH_4HSO_4 at uniaxial stresses 0.05 (a1,b1,c1) and 0.1 GPa (a2,b2,c2) near (a,b) T_1 and (c,d) T_2 without taking into account (a,c) and taking into account (b,d) the thermal expansion of the crystal lattice.

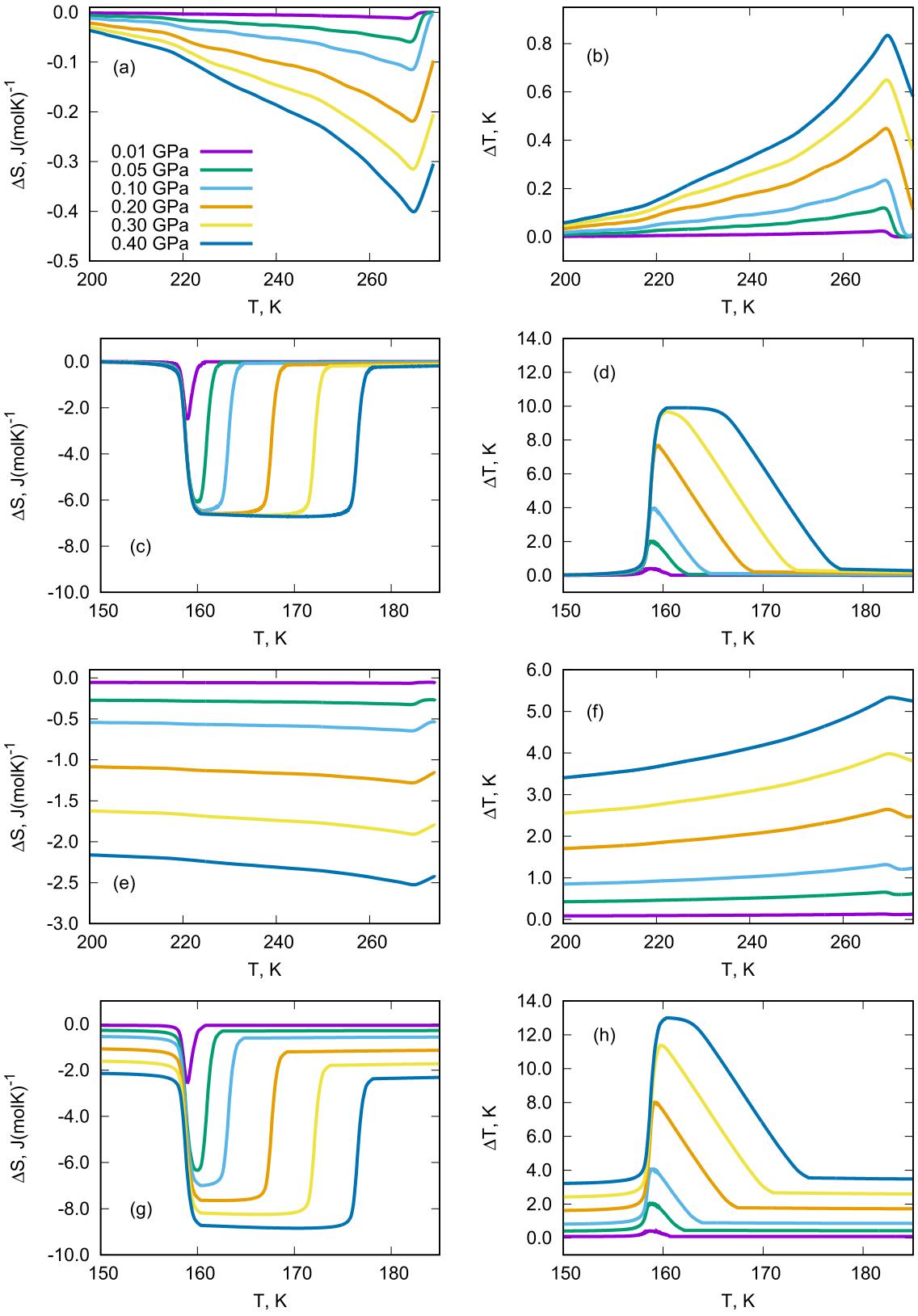

Fig. 4. Piezocaloric entropy ΔS_{PCE} and adiabatic temperature ΔT_{AD} changes at different uniaxial stresses σ_a in temperature regions near T_1 and T_2 without taking into account (a,b,c,d) and taking into account (e,f,g,h) the thermal expansion of the crystal lattice.

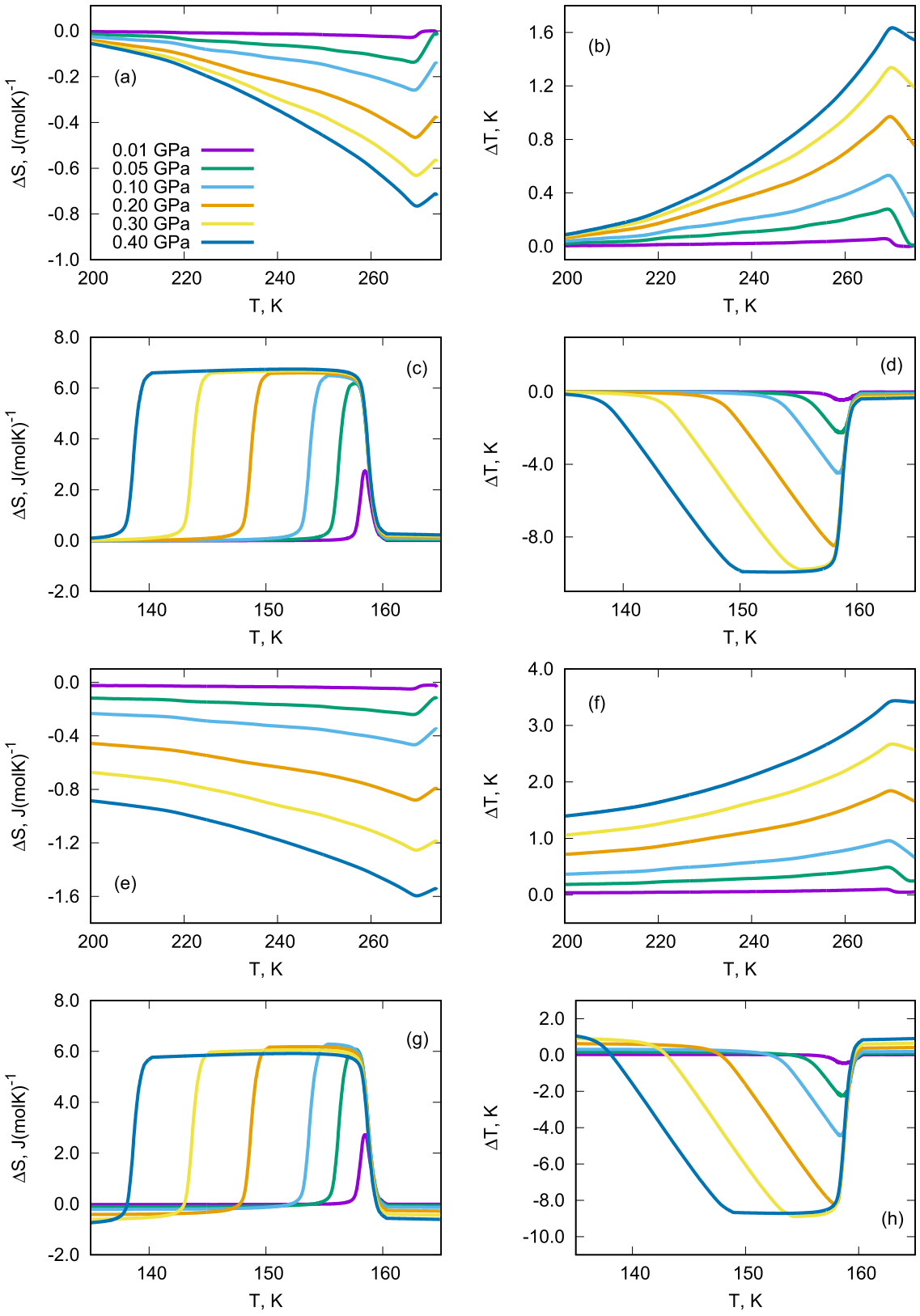

Fig. 5. Piezocaloric entropy ΔS_{PCE} and adiabatic temperature ΔT_{AD} changes at different uniaxial stresses σ_b in temperature regions near T_1 and T_2 without taking into account (a,b,c,d) and taking into account (e,f,g,h) the thermal expansion of the crystal lattice.

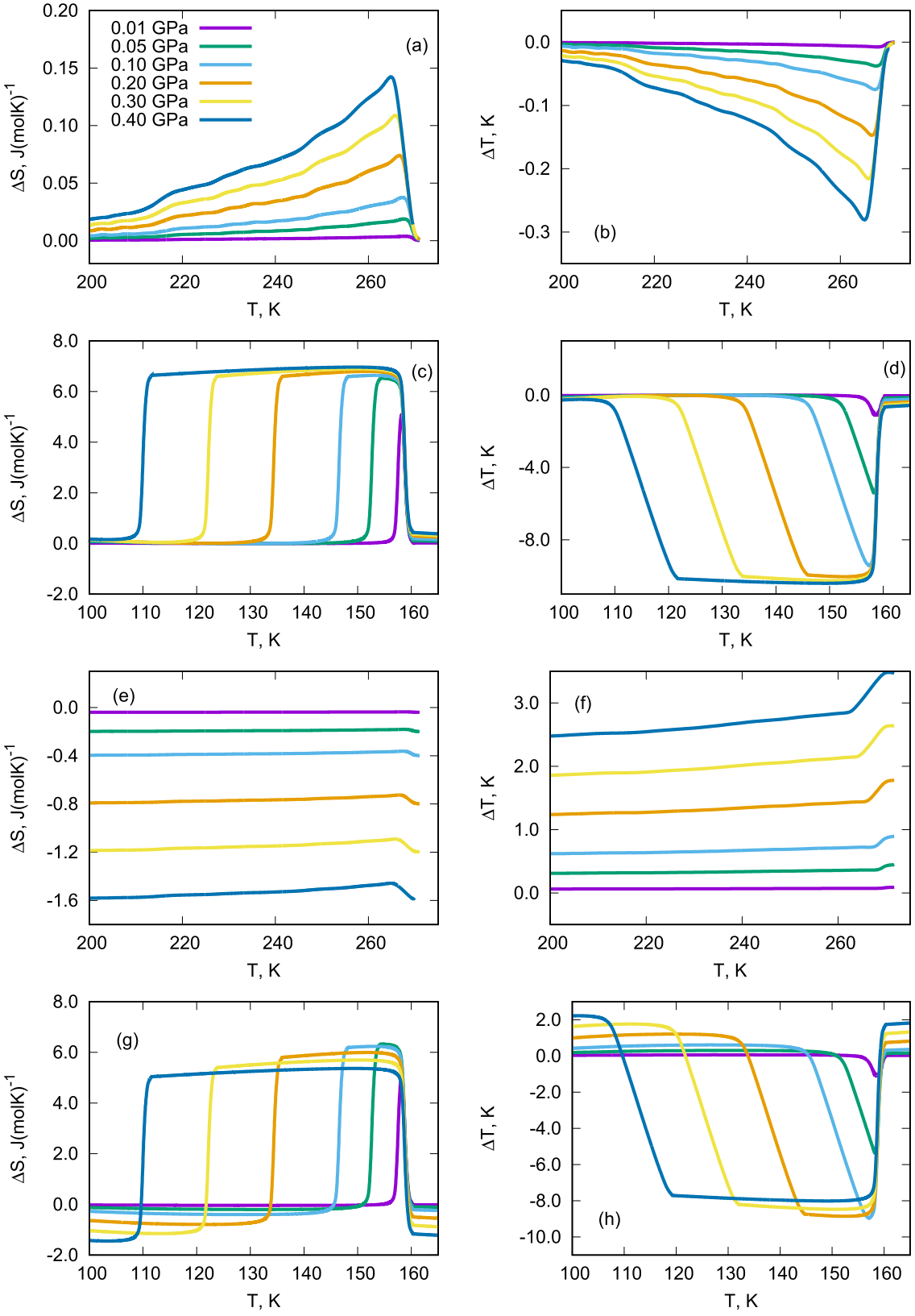

Fig. 6. Piezocaloric entropy ΔS_{PCE} and adiabatic temperature ΔT_{AD} changes at different uniaxial stresses σ_c in temperature regions near T_1 and T_2 without taking into account (a,b,c,d) and with taking into account (e,f,g,h) the thermal expansion of the crystal lattice.

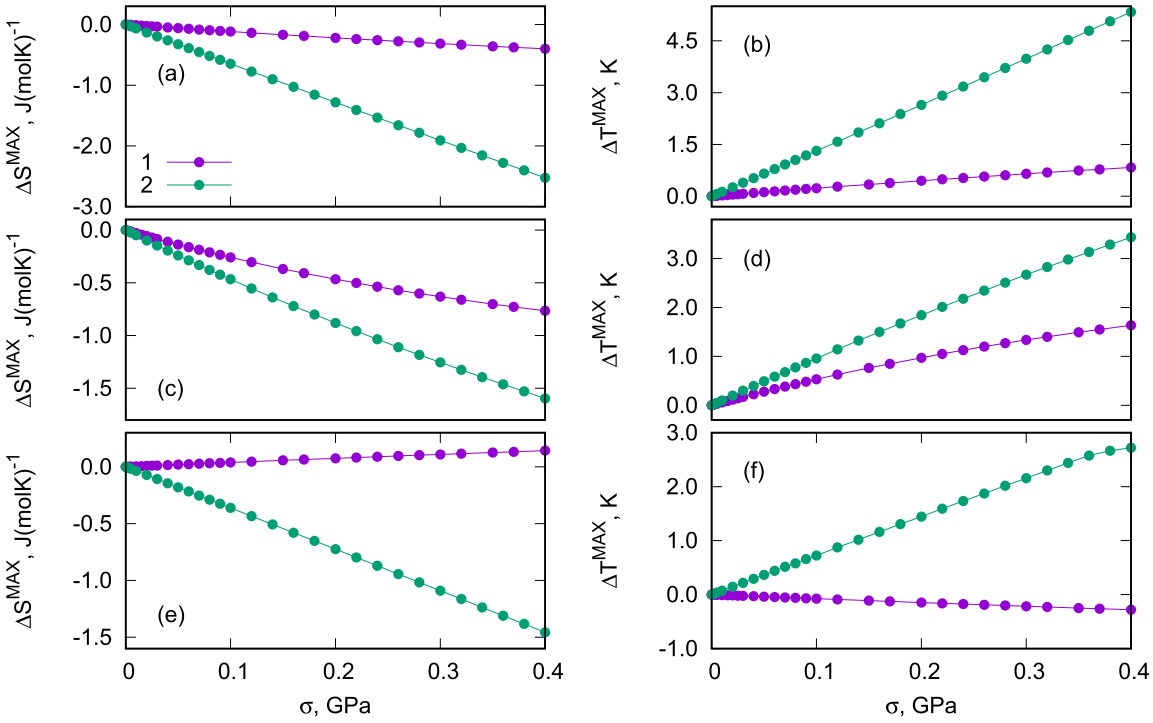

Fig. 7. The dependencies of ΔS_{PCE}^{max} and ΔT_{AD}^{max} on uniaxial stresses along *a*-axis (a,b), *b*-axis (c,d) and *c*-axis (e,f) near T_1 without (1) and with (2) taking into account the expansion of the crystal lattice.

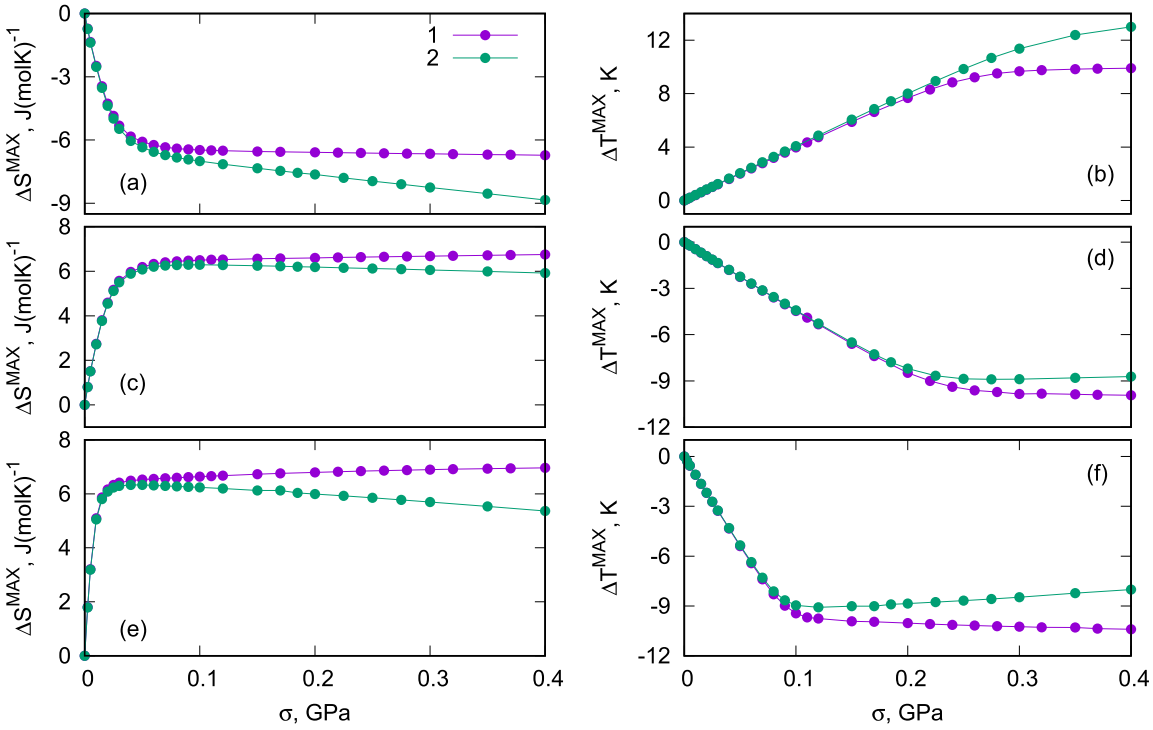

Fig. 8. The dependencies of ΔS_{PCE}^{max} and ΔT_{AD}^{max} on uniaxial stresses along *a*-axis (a,b), *b*-axis (c,d) and *c*-axis (e,f) near T_2 without (1) and with (2) taking into account the expansion of the crystal lattice.

Similar situation was observed at the phase transition $Pc \leftrightarrow P1$. Due to conventional origin of PCE associated with the positive sign of both α_a and $(\alpha_a)_{LAT}$, NH_4HSO_4 shows the most pronounced increase in the extensive and intensive effects associated with the *a* axis: the maximum values are equal to ΔS_{PCE}^{a} = -8.8 J/mol·K and ΔT_{AD}^{a} = 13 K at σ_a = 0.4 GPa (Fig. 4 (e), (g)). As to PCE along axes *b*

Table 2
Piezocaloric characteristics at phase transitions in materials of different physical origin.

	Sample	ΔS_{PCE}^{max}, J/kg·K	σ_i^{min}, GPa	ΔT_{AD}^{max}, K	σ_i^{min}, GPa	Ref.
$Cu_{68}Zn_{16}Al_{16}$	Polycr.			6–7	0.275	[28]
$Ni_{48.9}Ti_{51.1}$	Wire	46	0.8	25	0.8	[29]
$Ni_{35}Co_{15}Mn_{35}Ti_{15}$	Polycr.			9.0	0.6	[12]
$Ni_{50}Fe_{19}Ga_{27}Co_4$	Single cr.	15	0.3	10	0.3	[30]
$PbTiO_3$	Calculated			13	0.5	[20]
$PbTiO_3$	Calculated			20	0.8	[31]
$BaTiO_3$	Thin film			4.6	6	[18]
$(NH_4)_2NbOF_5$	Single cr.					[17]
c-axis		110	0.9	−16	0.9	
c-axis		−50	0.3	−7	0.3	
NH_4HSO_4 (at T_2)	Single cr.					This work
a-axis		−57	0.10	+10.0	0.30	
b-axis		+57	0.10	−10.0	0.30	
c-axis		+57	< 0.05	−10.0	0.10	

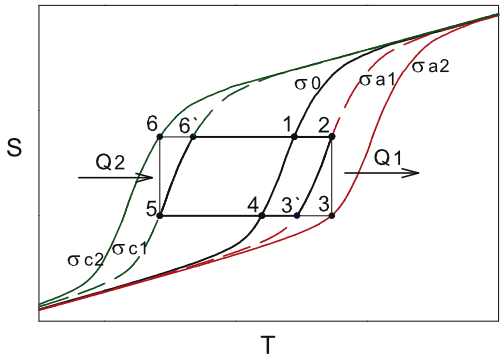

Fig. 9. Hypothetical cooling cycle 1-2-3′-4-5-6′-1 built on the combination of the piezocaloric effect associated with axes *a* and *c*. 1–3-4-5-6-1 cycle is the Carnot cycle with the same changes of entropy.

and *c*, different signs of $\alpha_b < 0$, $\alpha_c < 0$ and $(\alpha_b)_{LAT} > 0$, $(\alpha_c)_{LAT} > 0$ lead to decrease in both inverse effects and appearance of conventional contributions that increase with increasing pressure more faster in comparison with the decrease of inverse ΔS_{PCE} and ΔT_{AD} (Figs. 5 and 6).

It is interesting to consider the relation between the dependences of $\Delta S_{PCE}^{max}(\sigma_i)$ and $\Delta T_{AD}^{max}(\sigma_i)$ for all axes at both phase transitions without and with taking into account the expansion of the crystal lattice. At T_1, the behavior of both maximum effects is close to the linear (Fig. 7). However, it is necessary to be cautious about this situation, as we suggested that the uniaxial pressure used ($\sigma \leq 0.4$ GPa) does not affect the magnitude of the coefficients α and α_{LAT}.

Fig. 8 clearly demonstrates that at T_2, the maximum values of ΔS_{PCE} associated with each axis are realized at almost the same pressure. As to the values ΔT_{AD}^{max}, they can be achieved at rather different uniaxial pressure for different axes in accordance with a large difference in baric coefficients $dT/d\sigma_i$. In Fig. 8, the dependencies $\Delta S_{PCE}^{max}(\sigma_i)$ and $\Delta T_{AD}^{max}(\sigma_i)$ for *b* and *c* axes with taking into account the lattice contribution are shown only for the part of inverse PCE. This is the reason why both maximum values decrease with increasing pressure.

The data on PCE in NH_4HSO_4 are summarized in Table 2 in comparison with PCE in some other materials of the different origin.

One can see that the absolute maximum values of extensive and intensive effects are characteristic for different materials and can be realized with different mechanical stress σ. Very large value of ΔS_{PCE}^{max} in ferroelastic $(NH_4)_2NbO_2F_4$ observed under 0.9 GPa is a sum of two extensive effects associated with two temperature-close phase transitions [17]. When the uniaxial pressure decreases to the magnitude characteristic of PCE in NH_4HSO_4 at T_2, $\sigma = 0.1$–0.3 GPa, extensive effects in both materials become commensurate with each other. Large intense effect in a number of other materials was also observed under rather high pressure (Table 2).

Thus, due to the low pressure necessary for the realization of ΔS_{PCE}^{max} and ΔT_{AD}^{max}, ammonium hydrogen sulphate can be considered as a rather efficient solid-state coolant. Moreover, strong anisotropy of PCE allows the sample of NH_4HSO_4 to be heated or cooled by applying uniaxial pressure along different directions. Obviously this feature can be used to design a hypothetical combined refrigeration cycle built on alternate application of pressure along different crystallographic axes. In the case of the phase transition at T_2 in NH_4HSO_4, the combination of PCE associated with axes *a* and *c* looks the most promising.

Fig. 9 shows how a combined cycle can be organized. At the first stage, applying uniaxial pressure along the *a* axis in adiabatic process 1–2 leads to increase in temperature. During the process 2–3' ($\sigma_a = const$) heat transfers out from the refrigerant. Removal of σ_a (3–4, $S = const$) is accompanied by the decrease in temperature. Further cooling (4–5, $S = const$) is a result of applying pressure along the *c* axis, σ_c. In the process 5–6' ($\sigma_c = const$), heat transferred from the cooled reservoir to the refrigerant. Removal of σ_c (6' − 1, $S = const$) causes the system to return to initial state.

It is obvious that at the same entropy change in individual and combined cycles, the efficiency of the latter cycle is much higher due to a significant expansion of the working temperature range. Moreover, in this case the filling factor of the Carnot cycle 1-2-3-4-5-6-1 increases (Fig. 9).

Considered hypothetical cycle is also more convenient in comparison with the cycle based on a combination of two CE of different nature, ECE and PCE, recently analyzed [20]. One of the main reasons is that ECE is always accompanied by irreversible heating of the sample due to the release of Joule heat.

4. Conclusions

For the first time the effect of the anisotropy on caloric properties in ferroelectric material was studied and ammonium hydrogen sulphate was chosen as model object due to large difference in origin, type and sensitivity to external pressure of two structural transformations.

Dilatometric and X-ray measurements revealed a strong anisotropy of thermal expansion in the region of both phase transitions which led to a significant difference in the signs and values

of linear baric coefficients and as a result to anisotropy in piezocaloric properties. The greatest magnitudes of PCE at T_1 and T_2 are related to different axes and provide the main contribution to the barocaloric effect, considered as the sum of linear effects. The pressure behavior of the intensive and extensive PCE at the $P2_1/c \leftrightarrow Pc$ phase transition is close to the linear and as a result both of them do not show saturation even at $\sigma \approx 0.4$ GPa. At the same time, a strong nonlinearity of the dependences $\Delta S_{PCE}(\sigma_i)$ and $\Delta T_{AD}(\sigma_i)$ at the first order transformation $Pc \leftrightarrow P1$ leads to low mechanical stresses to achieve the maximum possible values of PCE. $\Delta S_{PCE}^{max} - \sigma_i = 0.05-0.10$ GPa and $\Delta T_{AD}^{max} - \sigma_i = 0.10-0.30$ GPa.

Taking into account the thermal expansion of the crystal lattice led to the greatest changes in PCE at T_1. The extensive effect equal to the entropy of the phase transition was achieved under rather low uniaxial pressure of 0.25–0.30 GPa. At T_2, the ΔS_{PCE} and ΔT_{AD} magnitudes associated with axis *a* and showing a conventional PCE increased by about 30% at $\sigma_a = 0.4$ GPa. Due to inverse PCE along *b* and *c* axes, these values were decreased.

Comparison of PCE in materials of different physical origin shows that NH_4HSO_4 can be considered as competitive solid refrigerant. Due to strong anisotropy of PCE, thermodynamic efficiency of the cooling cycle can be improved by alternate using uniaxial pressure along axes *a* and *c*.

Declaration of competing interest

XX The authors declare that they have no known competing financial interests or personal relationships that could have appeared to influence the work reported in this paper.

The authors declare the following financial interests/personal relationships which may be considered as potential competing interests:

CRediT authorship contribution statement

Ekaterina A. Mikhaleva: Formal analysis, Writing - original draft. **Mikhail V. Gorev:** Software. **Maxim S. Molokeev:** Investigation. **Andrey V. Kartashev:** Formal analysis, Investigation. **Igor N. Flerov:** Formal analysis, Conceptualization, Methodology.

Acknowledgements

The reported study was supported by the Russian Science Foundation (project no. 19-72-00023). X-ray and dilatometric data were obtained using the equipment of Krasnoyarsk Regional Center of Research Equipment of Federal Research Center “Krasnoyarsk Science Center SB RAS".

References

[1] Y.V. Sinyavskii, Electrocaloric refrigerators: a promising alternative to current low-temperature apparatus, Chem. Petrol. Eng. 31 (1995) 295–306, https://doi.org/10.1007/BF01148217.
[2] A.M. Tishin, Y.I. Spichkin, The Magnetocaloric Effect and its Applications, Institute of Physics Publishing, Bristol, United Kingdom, 2003.
[3] K.A. GschneidnerJr, V.K. Pecharsky, A.O. Tsokol, Recent developments in magnetocaloric materials, Rep. Prog. Phys. 68 (2005) 1479–1539, https://doi.org/10.1088/0034-4885/68/6/r04.
[4] S. Kar-Narayan, N.D. Mathur, Direct and indirect electrocaloric measurements using multilayer capacitors, J. Phys. D Appl. Phys. 43 (2010), https://doi.org/10.1088/0022-3727/43/3/032002, 032002.
[5] X. Moya, N.D. Kar-Narayan, S. andMathur, Caloric materials near ferroic phase transitions, Nat. Mater. 13 (2014) 439, https://doi.org/10.1038/nmat3951.
[6] A. Smith, C.R. Bahl, R. Bjørk, K. Engelbrecht, K.K. Nielsen, N. Pryds, Materials challenges for high performance magnetocaloric refrigeration devices, Adv. Energy Mater. 2 (2012) 1288–1318, https://doi.org/10.1002/aenm.201200167.
[7] P. Lloveras, A. Aznar, M. Barrio, P. Negrier, C. Popescu, A. Planes, L. Mañosa, E. Stern-Taulats, A. Avramenko, N.D. Mathur, X. Moya, J.-L. Tamarit, Colossal barocaloric effects near room temperature in plastic crystals of neopentylglycol, Nat. Commun. 10 (2019) 1803, https://doi.org/10.1038/s41467-019-09730-9.
[8] M. Valant, Electrocaloric materials for future solid-state refrigeration technologies, Prog. Mater. Sci. 57 (2012) 980–1009, https://doi.org/10.1016/j.pmatsci.2012.02.001.
[9] J.P. Joule, On some thermo-dynamic properties of solids, Phil. Trans. 149 (1859) 91–131.
[10] D. Soto-Parra, E. Vives, L. Mañosa, J.A. Matutes-Aquino, H. Flores-Zúñiga, A. Planes, Elastocaloric effect in Ti-Ni shape-memory wires associated with the B2 - B19' and B2 - R structural transitions, Appl. Phys. Lett. 108 (2016), https://doi.org/10.1063/1.4942009, 071902.
[11] C. Bechtold, C. Chluba, R. Lima de Miranda, E. Quandt, High cyclic stability of the elastocaloric effect in sputtered TiNiCu shape memory films, Appl. Phys. Lett. 101 (9) (2012), https://doi.org/10.1063/1.4748307, 091903.
[12] Z.Y. Wei, W. Sun, Q. Shen, Y. Shen, Y.F. Zhang, E.K. Liu, J. Liu, Elastocaloric effect of all-d-metal heusler NiMnTi(Co) magnetic shape memory alloys by digital image correlation and infrared thermography, Appl. Phys. Lett. 114 (2019) 101903, https://doi.org/10.1063/1.5077076.
[13] H. Sehitoglu, Y. Wu, E. Ertekin, Elastocaloric effects in the extreme, Scripta Mater. 148 (2018) 122–126, https://doi.org/10.1016/j.scriptamat.2017.05.017.
[14] B. Lu, J. Liu, Mechanocaloric materials for solid-state cooling, Sci. Bull. 60 (2015) 1638–1643, https://doi.org/10.1007/s11434-015-0898-5.
[15] L. Mañosa, A. Planes, Materials with giant mechanocaloric effects: cooling by strength, Adv. Mater. 29 (2017) 1603607, https://doi.org/10.1002/adma.201603607.
[16] M. Gorev, E. Bogdanov, I. Flerov, A. Kocharova, N. Laptash, Investigation of thermal expansion, phase diagrams, and barocaloric effect in the (NH4)2WO2F4 and (NH4)2MoO2F4 oxyfluorides, Phys. Solid State 52 (2010) 167–175, https://doi.org/10.1134/S1063783410010294.
[17] M. Gorev, E. Bogdanov, I. Flerov, N. Laptash, Thermal expansion, phase diagrams and barocaloric effects in (NH4)2NbOF5, J. Phys. Condens. Matter 22 (2010) 185901, doi:0953-8984/22/i=18/a=185901.
[18] Y. Liu, I.C. Infante, X. Lou, L. Bellaiche, J.F. Scott, B. Dkhil, Giant room-temperature elastocaloric effect in ferroelectric ultrathin films, Adv. Mater. 26 (2014) 6132–6137, https://doi.org/10.1002/adma.201401935.
[19] S. Patel, A. Chauhan, R. Vaish, Elastocaloric and piezocaloric effects in lead zirconate titanate ceramics, Energy Technol. 4 (2016) 647–652, https://doi.org/10.1002/ente.201500446.
[20] H. Khassaf, T. Patel, S.P. Alpay, Combined intrinsic elastocaloric and electrocaloric properties of ferroelectrics, J. Appl. Phys. 121 (2017) 144102, https://doi.org/10.1063/1.4980098.
[21] G. Bai, Q. Xie, J. Xu, C. Gao, Large negative piezocaloric effect: uniaxial stress effect, Solid State Commun. 291 (2019) 11–14, https://doi.org/10.1016/j.ssc.2019.01.002.
[22] Energy Savings Potential and RD&D Opportunities for Non-vapor-compression HVAC Technologies, Report of the U.S. Dpt. Of Energy, March 2014.
[23] E. Mikhaleva, I. Flerov, A. Kartashev, M. Gorev, E. Bogdanov, V. Bondarev, Thermal, dielectric and barocaloric properties of NH4HSO4 crystallized from an aqueous solution and the melt, Solid State Sci. 67 (2017) 1–7, https://doi.org/10.1016/j.solidstatesciences.2017.03.004.
[24] P. Lloveras, E. Stern-Taulats, M. Barrio, J.-L. Tamarit, S. Crossley, W. Li, V. Pomjakushin, A. Planes, L. Mañosa, N.D. Mathur, X. Moya, Giant barocaloric effects at low pressure in ferrielectric ammonium sulphate, Nat. Commun. 6 (2015) 8801, https://doi.org/10.1038/ncomms9801.
[25] R. Pepinsky, K. Vedam, S. Hoshino, Y. Okaya, Ammonium hydrogen sulfate: a new ferroelectric with low coercive field, Phys. Rev. 111 (1958) 1508–1510, https://doi.org/10.1103/PhysRev.111.1508.
[26] D. Swain, V.S. Bhadram, P. Chowdhury, C. Narayana, Raman and x-ray investigations of ferroelectric phase transition in NH4HSO4, J. Phys. Chem. A 116 (2012) 223–230, https://doi.org/10.1021/jp2075868.
[27] A.V. Kartashev, I.N. Flerov, N.V. Volkov, K.A. Sablina, Adiabatic calorimetric study of the intense magnetocaloric effect and the heat capacity of (La0.4Eu0.6)0.7Pb0.3MnO3, Phys. Solid State 50 (2008) 2115–2120, https://doi.org/10.1134/S1063783408110188.
[28] L. Mañosa, S. Jarque-Farnos, E. Vives, A. Planes, Large temperature span and giant refrigerant capacity in elastocaloric Cu-Zn-Al shape memory alloys, Appl. Phys. Lett. 103 (2013) 211904, https://doi.org/10.1063/1.4832339.
[29] J. Tušek, K. Engelbrecht, L.P. Mikkelsen, N. Pryds, Elastocaloric effect of Ni-Ti wire for application in a cooling device, J. Appl. Phys. 117 (2015) 124901, https://doi.org/10.1063/1.4913878.
[30] F. Xiao, M. Jin, J. Liu, X. Jin, Elastocaloric effect in Ni50Fe19Ga27Co4 single crystals, Acta Mater. 96 (2015) 292–300, https://doi.org/10.1016/j.actamat.2015.05.054.
[31] S. Lisenkov, B.K. Mani, C.-M. Chang, J. Almand, I. Ponomareva, Multicaloric effect in ferroelectric PbTiO3 from first principles, Phys. Rev. B 87 (2013) 224101, https://doi.org/10.1103/PhysRevB.87.224101.